Islamic University Journal of Applied Sciences (IUJAS)
https://journals.iu.edu.sa/jesc
Special Issue, February 2026, Pages 87-95
https://igee.univ-boumerdes.dz/ncaeee25/

Magnetothermal Analysis of Gold Melting in Crucible-Based Induction Furnaces Using Finite Volume Method

Zine Rezgui [1*], Sid-Ahmed Touil [2], Ammar Tibouche [1], Nabil Ikhlef [1]

[1]*Department of Electrical Engineering, Laboratory of electrical engineering and industrial electronics L2EI* University of Jijel, ALGERIA rezguizine73@gmail.com, tibouche_ammar@yahoo.fr, ikhlefnabil@yahoo.fr

[2]Institute of Electrical and Electronic Engineering, University of M'hamed BOUGARA - Boumerdes, ALGERIA s.touil@univ-boumerdes.dz

*Corresponding author: (Zine Rezgui), *Email Address*: rezguizine73@gmail.com

Abstract

This study examines the thermal and electromagnetic behavior of pure gold during induction heating, an area that has received limited research attention despite the widespread industrial use of induction technology for melting various metals. The research employs a finite volume computational method to analyze a 50 Hz crucible-based induction furnace [1], diverging from the finite element techniques typically used in previous investigations. The analysis focuses on determining the time and energy requirements needed to bring gold to its melting point of 1337.33 K, tracking the coupled magnetic and thermal processes throughout the heating cycle. The study presents theoretical foundations of electromagnetic and heat transfer principles. However, the modeling approach does not capture the actual melting transition or the coexistence of solid-liquid phases, as incorporating these phenomena would require advanced phase-change modeling and fluid dynamics calculations beyond the current scope.

Keywords: Induction heating, Gold, Magnetic process, Thermal process, Phase-change modeling,

https://doi.org/10.63070/jesc.2026.008
Received 25 November 2025; Revised 18 January 2026; Accepted 24 January 2026.
Available online 31 January 2026.
Published by Islamic University of Madinah on behalf of *Islamic University Journal of Applied Sciences*.
This is an open access article published under the Creative Commons Attribution 4.0 International license (CC BY 4.0):https://creativecommons.org/licenses/by/4.0/

1. Introduction

Induction heating represents a widely adopted industrial technology for metal processing, yet the specific thermal and electromagnetic characteristics of pure gold during induction melting have received comparatively limited research attention. This study addresses this gap by investigating the coupled magneto-thermal behavior of gold subjected to 50 Hz crucible-based induction heating, employing a finite volume computational approach that differs from the finite element methods predominantly used in the literature.

The research focuses on characterizing the time-dependent electromagnetic and thermal processes that occur as gold progresses from ambient conditions to its melting point of 1337.33 K. Understanding these coupled phenomena is essential for optimizing industrial induction melting operations, where energy efficiency and process control directly impact manufacturing economics and product quality.

Induction heating operates through electromagnetic induction, where alternating current flowing through a coil generates time-varying magnetic fields that induce eddy currents within electrically conductive workpieces. These induced currents encounter electrical resistance, generating volumetric heat through Joule heating. The process exhibits inherent complexity due to the interdependence of electromagnetic and thermal fields: material electrical conductivity varies with temperature, which in turn affects current distribution and heat generation patterns.

This investigation employs sequential coupling methodology to solve the governing electromagnetic and heat transfer equations using finite volume discretization. The approach tracks the evolution of magnetic vector potential distributions, induced current patterns, volumetric power dissipation, and temperature fields throughout the heating cycle [1]. Particular attention is given to the skin effect phenomenon, the tendency of alternating currents to concentrate near conductor surfaces which produces characteristic thermal gradients in the gold specimen.

The study provides theoretical foundations of the electromagnetic and heat transfer principles governing induction heating, presents the mathematical framework and numerical solution techniques, and analyzes the spatiotemporal behavior of key physical quantities during the heating process. While the current modeling approach does not incorporate phase-change phenomena or fluid dynamics associated with actual melting, it successfully predicts the energy requirements and temporal characteristics needed to bring gold to its fusion temperature, offering valuable insights for industrial furnace design and operation.

2. Mathematical Framework

Electromagnetic Theory

The mathematical modeling of induction heating can be simplified by neglecting charge distribution effects [2] and expressing the electromagnetic behavior solely through magnetic vector potential. For non-magnetic materials experiencing sinusoidal electromagnetic variations, the governing equation reduces to a more manageable form shown in Eq. (1),

$$Rot\left(Rot\left(\vec{A}\right)\right) + j\omega\sigma(T)\mu\vec{A} = \mu J_{ex} \qquad (1)$$

Where A represents the circumferential magnetic vector potential component (measured in *T.m*), *j* denotes the imaginary unit, ω indicates angular frequency (*rad/s*), σ represents electrical conductivity (*S/m*), and μ signifies magnetic permeability (*H/m*). The workpiece's electrical conductivity changes with temperature according to established relationships in references [3, 4], while the crucible is modeled with air-equivalent properties and the coil region excludes induced current effects by removing transient terms.

Heat Transfer Formulation

The thermal behavior during heating is captured through a transient diffusion equation (Eq. 2) that accounts for temperature-dependent material properties.

$$\rho(T)\,C(T)\,\frac{\partial T}{\partial t} = \nabla\cdot(k(T)\,\nabla T) + Q(T) \qquad (2)$$

With: $\boldsymbol{Q(T) = \frac{1}{2}\sigma(T)\omega^2 AA^*}$.

In this formulation, *T* denotes temperature (*K*), ρ represents density (kg/m^3), *C* indicates specific heat capacity (*J/(kg.K)*), *k* signifies thermal conductivity (*W/(m.K)*), and *Q* represents internal heat generation (W/m^3) derived from the electromagnetic solution through the complex conjugate of the magnetic vector potential *A**. Both the crucible and gold workpiece exhibit temperature-dependent variations in their thermal properties ρC and *k* [3, 5-7].

Henceforth, for notational convenience, we omit the temperature dependence term and simply write instead σ of $\sigma(T)$, with similar notation for ρC and *k* and *Q*.

Coupled Magnetothermal Numerical Technique

Electromagnetic Modeling

The magneto-dynamic equation for axisymmetric geometries in cylindrical coordinates takes the form shown in Eq. (3). The finite volume method divides the computational domain into discrete cells [1].

$$-\frac{\partial^2 A}{\partial z^2}+\frac{A}{r^2}-\frac{1}{r}\frac{\partial}{\partial r}\left(r\frac{\partial A}{\partial r}\right)+j\omega\sigma\mu A=\mu J_{ex} \quad (3)$$

The spatial derivatives are converted to algebraic differences between nodal values through standard integration procedures. Assuming uniform grid spacing and applying appropriate algebraic operations, the continuous differential equation reduces to a discrete five-point formula given by Eq. (4),

$$a'_p A_p = a'_e A_E + a'_w A_W + a'_n A_N + a'_s A_S + b'_p \quad (4)$$

Where:

$a'_e = \frac{r_e \Delta z}{\Delta r}$, $a'_w = \frac{r_w \Delta z}{\Delta r}$, $a'_n = \frac{r_p \Delta r}{\Delta z}$, $a'_s = \frac{r_p \Delta r}{\Delta z}$,

$a'_p = a'_e + a'_w + a'_n + a'_s + j\omega\sigma_p \mu r_p \Delta r \Delta z + \ln\left(\frac{r_e}{r_w}\right)\Delta z$ and $b'_p = \mu J_{ex} r_p \Delta r \Delta z$

Here, in represents the natural logarithm function.

Where coefficients $a'_e, a'_w, a'_n, a'_s, and\ b'_p$ are defined in terms of mesh dimensions, material properties, and excitation current density.

Heat Transfer Modeling

For axisymmetric problems where temperature varies only with radial and axial coordinates, the thermal diffusion equation simplifies to Eq. (5).

$$\rho C\frac{\partial T}{\partial t}=\frac{1}{r}\frac{\partial}{\partial r}\left(rk\frac{\partial T}{\partial r}\right)+\frac{\partial}{\partial z}\left(k\frac{\partial T}{\partial z}\right)+Q \quad (5)$$

Although electromagnetic calculations encompass the entire domain including the coil, thermal analysis is restricted to the workpiece and crucible regions based on physical relevance [1, 2]. The discretization strategy follows the finite volume approach [1, 8, 9], integrating Eq. (5) over both the control volume and time interval to produce Eq. (6).

$$\int_t^{t+\Delta t}\int_s^n\int_w^e \rho C\frac{\partial T}{\partial t}2\pi r dr dz\, dt = \int_t^{t+\Delta t}\int_s^n\int_w^e \frac{1}{r}\frac{\partial}{\partial r}\left(rk\frac{\partial T}{\partial r}\right)2\pi r dr dz dt + \int_t^{t+\Delta t}\int_s^n\int_w^e \frac{\partial}{\partial z}\left(k\frac{\partial T}{\partial z}\right)2\pi r dr dz\, dt + \int_t^{t+\Delta t}\int_s^n\int_w^e Q 2\pi r dr dz\, dt \quad (6)$$

An implicit time-marching scheme is employed to ensure computational stability and accuracy. Under uniform mesh spacing assumptions, these manipulations culminate in the discrete five-point stencil

formula shown in Eq. (7), with coefficients $\boldsymbol{a'_e, a'_w, a'_n, a'_s, and\ b'_p}$ defined based on thermal properties, mesh parameters, and time step size.

$$a_p T_p^{n+1} = a_e T_E^{n+1} + a_w T_W^{n+1} + a_n T_N^{n+1} + a_s T_S^{n+1} + b_p \qquad (7)$$

Where: $a_e = \frac{r_e k_e \Delta z}{\Delta r}$, $a_w = \frac{r_w k_w \Delta z}{\Delta r}$, $a_n = \frac{r_p k_n \Delta r}{\Delta z}$, $a_s = \frac{r_p k_s \Delta r}{\Delta z}$, $a_p = a_e + a_w + a_n + a_s + \frac{\rho C_p r_p \Delta r \Delta z}{\Delta t}$,

and $b_p = Q_p r_p \Delta r \Delta z + \frac{\rho C_p r_p \Delta r \Delta z}{\Delta t} T_p^n$

The Gauss-Seidel iterative technique is applied to solve both electromagnetic and thermal algebraic equation systems.

Coupling Strategies for Electromagnetic-Thermal Analysis

This section examines two primary methodologies for simulating systems involving electromagnetic and thermal interactions. The direct approach integrates both phenomena into a unified solution framework, while the sequential method treats them as separate but interconnected processes solved iteratively. Although direct coupling provides comprehensive simultaneous solutions, it demands extensive computational resources requiring five simultaneous variables per discretized element. Given these resource constraints, direct methods warrant application only when physical conditions strictly require such treatment. This work adopts the sequential approach, offering an effective compromise between numerical efficiency and accurate physical representation of coupled phenomena.

System Configuration and Operating Parameters for Gold Induction Melting

This investigation focuses on an induction heating system designed to melt pure gold contained within an alumina crucible. The experimental setup utilizes a cylindrical ceramic vessel with 100 mm internal diameter, 100 mm height, and 10 mm thick walls, loaded with gold measuring 100 mm in diameter and 90 mm in height. A single-turn copper conductor with rectangular profile serves as the heating coil, positioned 5 mm from the crucible surface. The system operates at standard power frequency (50 Hz) with a coil current density of 6.17×10^8 A/m², generating electromagnetic fields sufficient to raise the gold temperature to its liquefaction point of 1337.33 K. The computational model extends 100 mm beyond the coil's outer boundary to capture the complete electromagnetic field distribution.

The physical configuration examined and the imposed boundary specifications appear in Fig. 1.

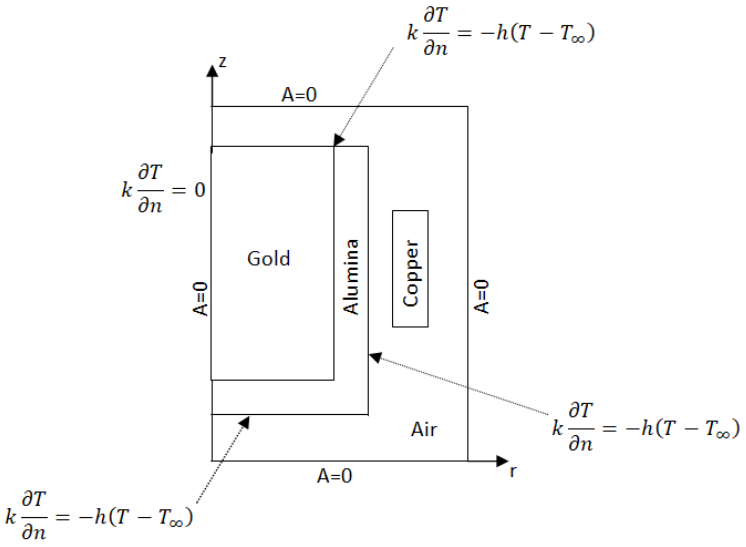


Fig. 1. Physical configuration and boundary specifications.

3. Results and Discussion

Study of Temperature Distributions

This analysis investigates how thermal fields develop over time throughout the induction heating cycle [1]. During the initial 60-second phase, electromagnetic power concentrates primarily at the gold specimen's exterior surface, creating steep radial thermal gradients Fig. 2. The outer regions experience accelerated temperature rise while interior zones remain comparatively cold, a consequence of electromagnetic skin depth limitations in conductive materials. Beyond one minute of operation, heat diffusion becomes the dominant transport mechanism. Gold's superior thermal transport coefficient (approximately 317 W/m.K at room temperature) enables effective radial heat migration from hot exterior surfaces toward cooler central regions, progressively equalizing the temperature distribution throughout the specimen volume.

This two-stage behavior, initial surface heating followed by conductive redistribution, characterizes the temporal dynamics of electromagnetic induction melting processes.

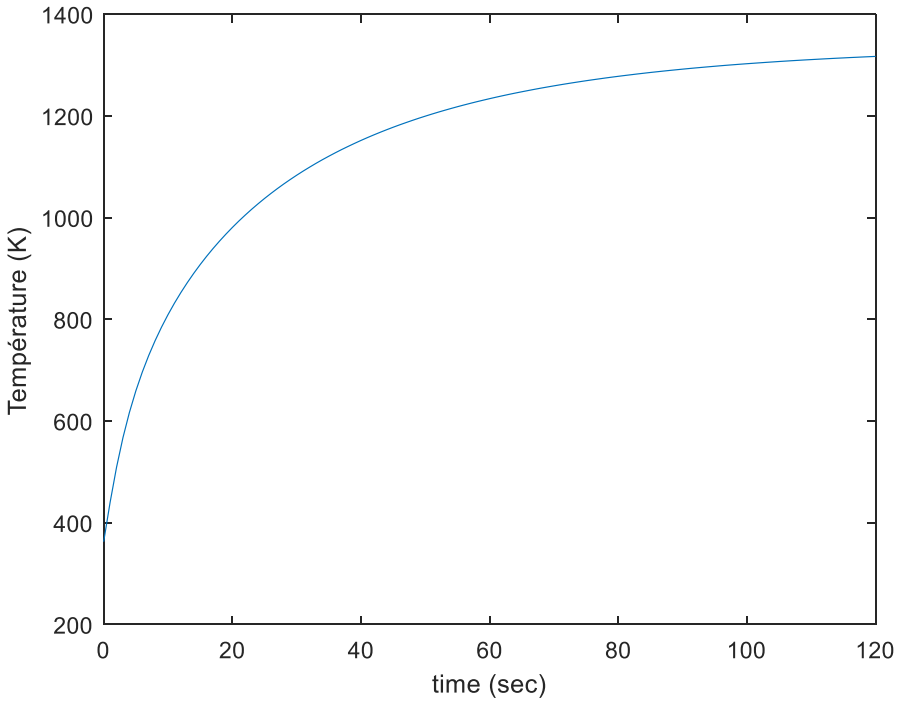


Fig. 2. Temperature evolution with time at the mid-point of the load.

Spatiotemporal Behavior of the magnetic vector potential A

This section examines the magnetic vector potential A, which serves as the fundamental electromagnetic quantity from which electric and magnetic fields are derived. The vector potential maintains remarkable spatiotemporal consistency throughout the heating process. Its spatial distribution exhibits a bell-shaped axial profile concentrated in the primary coupling region Fig. 3, accompanied by an exponential decay pattern in the radial direction Fig. 4. Temporal variations prove minimal, with fluctuations on the order of 10^{-6} in the axial direction and 10^{-4} to 10^{-5} radially, representing the most stable parameter among all measured quantities. This near-constant behavior contrasts sharply with its derivatives (induced currents and volumetric power dissipation), which demonstrate significant time-dependent changes. The phenomenon reveals a fundamental characteristic of induction systems: the primary electromagnetic driver remains essentially invariant while generating substantial variations in secondary electromagnetic effects [1].

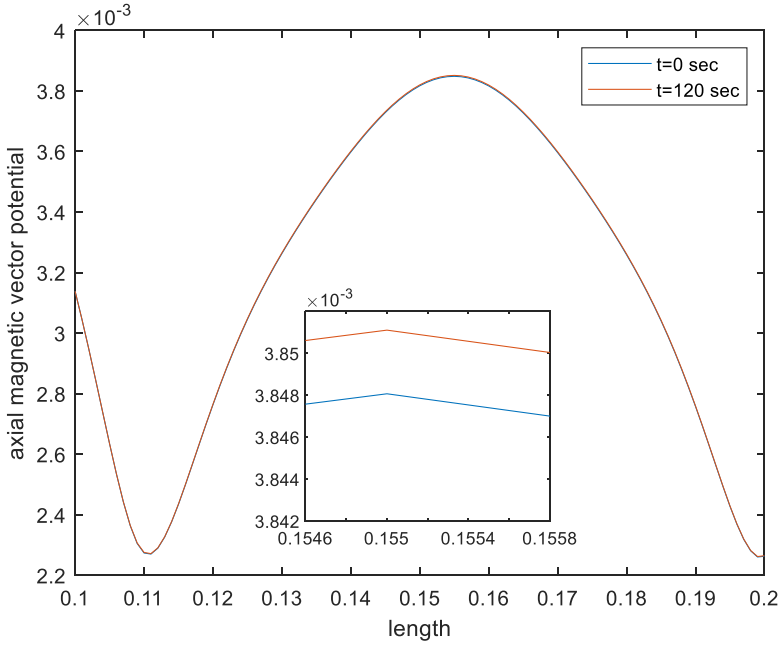


Fig. 3. Magnetic vector potential in the axial direction.

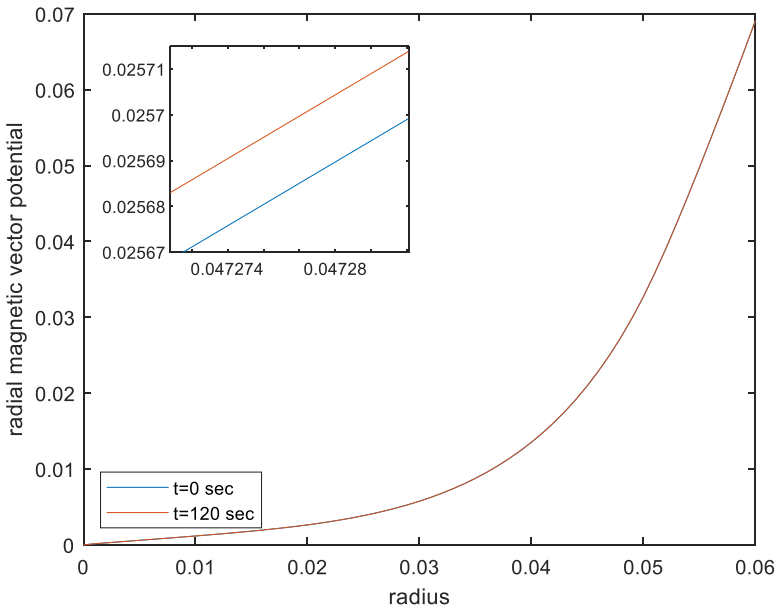


Fig. 4. Magnetic vector potential in the radial direction.

4. Conclusion

This research presents a finite volume numerical framework for analyzing coupled electromagnetic and thermal physics in 50 Hz induction melting of gold. Results demonstrate that skin effect produces steep radial thermal gradients, with outer surfaces heating considerably faster than interior regions [1]. Despite gold's excellent heat conduction properties (thermal conductivity near 317 W/m•K), complete thermal uniformity remains unattainable due to persistent electromagnetic heating at the surface. The sequential coupling methodology delivers computational efficiency while accurately predicting temporal and energy requirements for reaching gold's fusion temperature (1337.33 K). A striking contrast emerges between electromagnetic field behavior where electric field, magnetic field, and vector potential display spatial consistency with negligible temporal drift and thermal response, which evolves dynamically throughout the process. These findings illuminate the intricate relationship between quasi-steady electromagnetic forcing and time-dependent thermal response mechanisms inherent to induction heating technology.

References

[1] Rezgui, Z., Tibouche, A., & Ikhlef, N. (2025). Numerical investigation of gold melting in an induction crucible furnace: a parametric study of electromagnetic and thermal characteristics using finite volume method. *Gold Bulletin*, *58*(1), 11.

[2] Rudnev, V., & Totten, G. E. (Eds.). (2014). Induction heating and heat treatment. ASM international.

[3] Auerkari, P. (1996). Mechanical and physical properties of engineering alumina ceramics (Vol. 23). Espoo, Finland: Technical Research Centre of Finland.

[4] Rudnev, V., Loveless, D., & Cook, R. L. (2017). Handbook of induction heating. CRC press.

[5] VUILLERMOZ, P. L., & LAURENT, M. (1993). *Conductivité thermique des solides*. Ed. Techniques Ingénieur.

[6] Khvan, A. V., Uspenskaya, I. A., Aristova, N. M., Chen, Q., Trimarchi, G., Konstantinova, N. M., & Dinsdale, A. T. (2020). Description of the thermodynamic properties of pure gold in the solid and liquid states from 0 K. Calphad, 68, 101724.

[7] Arblaster, J. W. (2016). Thermodynamic properties of gold. *Journal of Phase Equilibria and Diffusion*, *37*(2), 229-245.

[8] Mazumder, S. (2015). Numerical methods for partial differential equations: finite difference and finite volume methods. Academic Press.

[9] Murthy, J. Y., & Mathur, S. R. (2002). Numerical methods in heat, mass, and momentum transfer. School of Mechanical Engineering Purdue University.